Catalysis Communications 34 (2013) 35–40

Contents lists available at SciVerse ScienceDirect

Catalysis Communications

journal homepage: www.elsevier.com/locate/catcom

Short Communication

# Antibacterial activity of photocatalytic electrospun titania nanofiber mats and solution-blown soy protein nanofiber mats decorated with silver nanoparticles

Yiyun Zhang [a,1], Min Wook Lee [b,1], Seongpil An [b], Suman Sinha-Ray [a], Shahrzad Khansari [a], Bhavana Joshi [b], Seungkwan Hong [c], Joo-Hyun Hong [d], Jae-Jin Kim [d], B. Pourdeyhimi [e], Sam S. Yoon [b,*], Alexander L. Yarin [a,**]

[a] Department of Mechanical and Industrial Engineering, University of Illinois at Chicago, 842W. Taylor St., Chicago, IL 60607-7022, USA
[b] School of Mechanical Engineering, Korea University, Seoul, 136-713, Korea
[c] School of Civil, Environmental & Architectural Engineering, Korea University, Seoul 136-713, Korea
[d] Department of Environmental Science & Ecological Engineering, Korea University, Seoul, 136-713, Korea
[e] 3427 The Nonwovens Institute, Box 8301, North Carolina State University, Raleigh, NC 27695-8301, USA

ARTICLE INFO

*Article history:*
Received 18 October 2012
Received in revised form 7 January 2013
Accepted 7 January 2013
Available online 15 January 2013

*Keywords:*
Antibacterial
Electrospinning
Titania
Soy protein
Solution blowing
Silver nanoparticles

ABSTRACT

Highly porous photocatalytic titania nanoparticle decorated nanofibers were fabricated by electrospinning nylon 6 nanofibers onto flexible substrates and electrospraying $TiO_2$ nanoparticles onto them. Film morphology and crystalline phase were measured by SEM and XRD. The titania films showed excellent photokilling capabilities against *E. coli* colonies and photodegradation of methylene blue under moderately weak UV exposure ($\leq$ 0.6 mW/cm$^2$ on a 15-cm illumination distance). In addition, solution blowing was used to form soy protein-containing nanofibers which were decorated with silver nanoparticles. These nanofibers demonstrated significant antibacterial activity against *E. coli* colonies without exposure to UV light. The nano-textured materials developed in this work can find economically viable applications in water purification technology and in biotechnology. The two methods of nanofiber production employed in this work differ in their rate with electrospinning being much slower than the solution blowing. The electrospun nanofiber mats are denser than the solution-blown ones due to a smaller inter-fiber pore size. The antibacterial activity of the two materials produced (electrospun titania nanoparticle decorated nanofibers and silver-nanoparticle-decorated solution-blown nanofibers) are complimentary, as the materials can be effective with and without UV light, respectively.



## 1. Introduction

Water pollution and shortage pose serious environmental problems worldwide, and interests in water purification or antibacterial treatments are growing substantially. Antimicrobial functionalities in water filtration are required in multiple applications, starting from membranes used in construction industry to bandages used for wound healing. For this reason, fabrication of antibacterial materials has become one of the most challenging global research issues [1–3]. Nanoparticles have recently gained significant attention due to their high surface to volume ratio which leads to specific characteristics that differ from bulk material. Both semiconducting ceramic and metal nanoparticles are of interest due to their potential to act as antibacterial. In previous studies [4,5], it was shown that such metals as silver, titanium, zinc, and calcium act as antimicrobial agents, while titanic oxide, tin oxide, and silver oxide have also been proven to be potential antibacterial ceramic materials [6,7]. In particular, these metals and ceramics are sources of cations that react with hydroxyl and anionic groups of enzymes in bacteria which results in change of functionalization in bacterial cells. Of all metal particles, silver has shown the strongest antibacterial effect which has been investigated vastly [4,5]. As a result, silver nanoparticle-coated surfaces made their way into cosmetics, textile, and pharmaceutical products. Growing interest in functionalizing silver nanoparticles for different applications brought about toxicity issue of these particles, yet it has been documented that moderate usage of silver in human's body would not have a major reverse impact [8]. As for the ceramic nanoparticles, $TiO_2$ has been proven to be the most promising photokilling material because of its ability to generate hydroxyl

* Corresponding author at: S.S. Yoon, School of Mechanical Engineering, Korea University, Seoul, 136-713, Korea. Tel.: +82 2 3290 3376; fax: +82 2 926 9290.
** Correspondence to: A.L. Yarin, Department of Mechanical and Industrial Engineering, University of Illinois at Chicago, 842 W. Taylor St., Chicago, IL 60607-7022, USA. Tel.: +1 312 996 3472; fax: +1 312 413 0447.
*E-mail addresses:* skyoon@korea.ac.kr (S.S. Yoon), ayarin@uic.edu (A.L. Yarin).
[1] Equal contribution.

1566-7367/$ – see front matter © 2013 Elsevier B.V. All rights reserved.
http://dx.doi.org/10.1016/j.catcom.2013.01.002

radicals upon receiving UV-light [9]. Antibacterial activity of $TiO_2$ must be activated by UV while UV is not necessary for antibacterial activity of silver. The combination of the superior hydrophilicity and photokilling effect of $TiO_2$ led to its usage in water purification, medical applications [7], odor elimination, decoloring wastewater [10,11], mineralization of both hazardous organic and inorganic materials [12,13], soil decontamination [14], destruction of cancer cells and viruses [15], and medical sterilization.

The use of nanoparticles for antibacterial application is often difficult, e.g. for water purification, nanoparticles should be dispersed in a polluted aqueous medium to make best usage of their high surface to volume. However, the subsequent separation of nanoparticles from purified water is difficult as they remain in a colloidal state and do not sufficiently settle. As a result, an additional equipment is required [16]. In lieu of this, an immobilized mode, or fabrication of films is often proposed as an alternative. However, this immobilized mode prevents the effective usage of nanoparticles by compacting them into a two-dimensional film which dramatically reduces the interfacial contact between nanoparticles the polluted medium. Antibacterial treatments imply a significant area of contact of an active material with polluted medium. Nano-textured materials with open porosity, such as electrospun or solution-blown nanofiber mats possess specific surface area in the range 10–100 $m^2/g$, which makes them attractive candidates for nanoparticle supports in water purification processes [4,5,17]. In addition, nanofibers can be used as filters as pores with sizes in the range ~1–10 μm can catch pollutants more efficiently than standard filters [18]. In addition to filtration, nanofibers are also shown to be effective for wound dressing [19,20]. Nanofibers with antimicrobial functionalities can facilitate development of very efficient membranes. In this respect, $TiO_2$ and silver nanoparticles represent themselves as two best possible candidates because $TiO_2$ can perform in the presence of UV light, whereas silver is active without UC light due to its intrinsic antimicrobial capability.

In this work, we form and test two model types of the antibacterial materials. The first one is solution-blown soybean-nylon nanofiber mats decorated with silver nanoparticles. Their antibacterial effect does not require UV illumination. We also form and test the antibacterial effect of electrospun nylon nanofiber mat decorated with $TiO_2$ nanoparticles. Such nanofiber mats become bioactive upon UV illumination. This allows us to introduce such novel biocatalyst supports which can be active with or without UV light, or both with and without UV light when silver and $TiO_2$-coated nanofibers are used simultaneously.

## 2. Experimental

### 2.1. Preparation of nanofiber

#### 2.1.1. Electrospinning of titania nanoparticle decorated nanofiber

Fig. 1 shows the process of titania-decorated nanofiber mat fabrication. Agglomerated $TiO_2$ nano-particles (P25-Daegusa, Germany) are a mixture of 80% anatase and 20% rutile, whose actual size was in the range of micro-scale because of severe agglomeration, and are dispersed in ethanol solution to facilitate electrospray deposition onto flexible glass substrates attached to the cylinder rotating at 300 RPM. Polymer solution (15 wt.% nylon 6 dissolved in formic acid, *Sigma Aldrich*) was horizontally electrospun onto a rotating cylinder to produce nanofibers. $TiO_2$ nanoparticles were sprayed from the top on the nanofibers for 5 minutes (cf. Fig. 1). Nylon fibers of high strength are to firmly hold $TiO_2$ nanoparticles. Nozzles used for both electrospraying and electrospinning had the diameter of 4 mm and 0.84 mm, respectively. In electrospinning the dc voltage applied was $V_1 = 7$ kV and $V_2 = 9$ kV for flow rates of $Q_1 = 1$ ml/h and $Q_2 = 0.1$ ml/h, respectively; see Fig. 1. The nozzle-to-substrate distances, $S_1$ and $S_2$, are important process parameters. Their optimal values were found at $S_1 = 2$ cm and $S_2 = 6$ cm, which yields a uniform distribution that minimizes agglomeration of $TiO_2$ nanoparticles. Readers are referred to our previous study [21] regarding detailed preparations of photodegradation of methylene blue (MB) and bacterial growth media.

#### 2.1.2. Soy protein materials

Materials used in this work are as follows. Soy protein isolate-PRO-FAM 955 (SP 955) was provided by ADM Specialty Food Ingredients. Polyamide-6 (Nylon-6) ($M_w = 65.2$ kDa) was obtained from BASF.

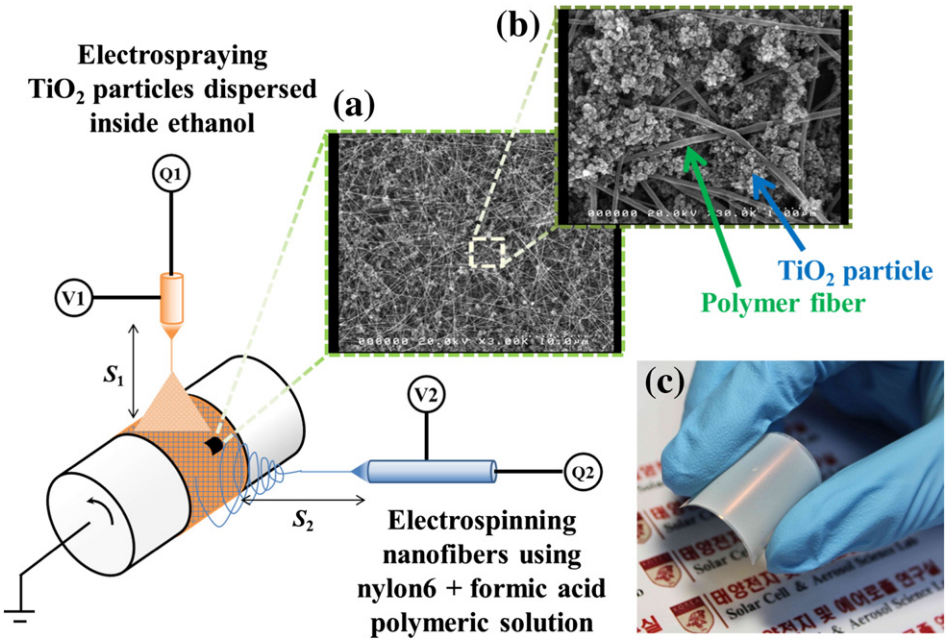


**Fig. 1.** Fabrication of titania-decorated nanofiber mat via electrospinning polymer solution and electrospraying $TiO_2$ nanoparticles. (a) SEM image showing suspended $TiO_2$ nanoparticles between nanofibers. (b) Magnified view of nanoparticles and nanofibers. (c) Snapshot of the titania-decorated nanofiber mat. In the experiments $S_1 = 2$ cm and $S_2 = 6$ cm.

Formic acid (grade > 95%), silver nitrate ($AgNO_3$), and sodium borohydride ($NaBH_4$) were purchased from Sigma-Aldrich. *Escherichia coli* (Migula) Castellani and Chalmers (ATCC 25922) were obtained from the American Type Culture Collection (ATCC). Trypticase soy agar and trypticase soy broth were purchased from Cole- Parmer.

*2.1.3. Soy protein solution preparation*

For solution blowing, 1.0 g SPI was mixed with 9.5 g formic acid and left on a hotplate at 75 °C for 24 h. Next, 1.5 g nylon 6 was mixed with this solution. The mixture was left on the hotplate for another day at the same temperature. For decorating soy protein-containing nanofibers with silver, a 1% $AgNO_3$ solution in de-ionized water was prepared. The solution was sonicated for 30 min to make it homogeneous. Also, a 1% sodium borohydride solution in de-ionized water was prepared by sonicating for 30 min.

*2.1.4. Solution blowing of soy protein-containing nanofibers*

Soy protein isolate/nylon 6 blend in formic acid was solution blown as described in the previous studies [22,23]. In brief, the solution was pumped into a 13G needle that was surrounded by an annular nozzle through which turbulent air jet was issued. The solution flow rate through the needle was kept at 5.0 ml/h during the experiment and the upstream pressure of air was set at 2.0 bar. The polymer solution jet issued from the needle was stretched and bent, and thus thinned, by the surrounding air jet. As a result, nanofibers with an average diameter of 300–500 nm were produced. Solution-blown nanofibers were then collected on an aluminum rotating drum with the linear velocity of about 3.0 m/s on the drum surface.

*2.2. Characterization*

The microstructures and crystallinity of the $TiO_2$-decorated nanofiber mats were characterized by both high-resolution scanning electron microscopy (Hitachi S-5000) and X-ray diffraction (XRD, *Rigaku Japan*, D/MAX-2500) using Cu Kα radiation over a 2θ range of 20° to 50°. Scanning electron microscopy of silver coated soy based solution blown nanofiber was done using Hitachi S-3000N variable pressure SEM.

## 3. Results and discussion

*3.1. Titania-decorated nanofibers*

SEM images of the titania decorated nanofibers are shown in Fig. 1. It can be seen that titania nanoparticle formed agglomerate on the nanofiber mat. Porosity of the electrospun nanofiber mat was estimated to be approximately 38%, which was obtained by counting the void pixels from the 2D SEM image. It should be mentioned that the composite fiber mat was collected on a flexible substrate. It could be bent as shown in Fig. 1 without causing any delamination of nanoparticles from the fiber mat, which clearly shows that electrosprayed titania nanoparticles adhere tightly to the electrospun nanofibers. Furthermore, the mat was sonicated inside an ultrasonic bath for a few minutes and yet the internal microstructure of the mat remained the same, indicating the structural stability of the mat. However, it should be noted that after tens of UV irradiation hours (i.e., 10–24 h), the nylon nanofibers were degraded due to the photocorrosion effect. The fibers may be replaced by other photo-resistant polymeric materials if desired for specific applications.

Fig. 2 displays the effect of UV exposure on MB photo-degradation in terms of absorbance data over a wavelength range 400 − 800 nm for various durations of UV irradiation: $t_{UV} = 0$, 30, 60, and 90 min. The greater the intensity of the transmitted light, the lower the absorbance. A lower absorbance is indicative of an increased photo-degradation of the MB solution. The inset in Fig. 2 is a snapshot of the photo-induced degradation of the MB solution corresponding to the data in Fig. 2. The far-right snapshot shows a nearly transparent

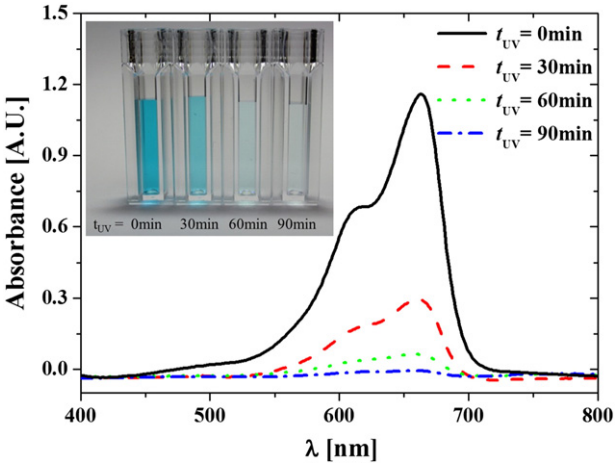


**Fig. 2.** Absorbance transition for several values of the duration of UV irradiation, $t_{UV}$.

MB solution, which indicates a successful photodegradation process. The highest absorbance peak is observed at λ ≈ 664 nm [24], which decreases as the photocatalytic reaction proceeded with $t_{UV}$. Peak reduction is caused by photo-oxidative N-demethylation of MB [25,26].

Fig. 3 displays photographs of Petri dishes with *E. coli* colonies (white spots) used in the bactericidal test. Photokilling or antibacterial activity was measured by comparing the number of surviving *E. coli* bacteria colonies on the non-coated and titania-coated substrates. Four cases are considered herein: (a) a case without titania coating and no UV light, (b) a case with titania coating without UV light, (c) a case without titania coating and with UV light, and (d) a case with titania coating and with UV light. Because UV exposure itself without titania photocatalysis is capable of killing bacteria, the sole effect of UV illumination should also be quantified, which is the case in (c).

For substrates without titania coating, the effect of UV light alone is quantified by comparing Figs. 3(a) and (c); there was appreciable photokilling activity of the UV-light (0.6 mW/cm$^2$ on a 15-cm illumination distance, 365 nm) as the number of surviving bacterial colonies changed from 1377 to 1109; thus, the UV effect is present but minor. By comparing Figs. 3(b) and (d), not only the UV effect, but also that of $TiO_2$ photokilling activity is also quantified; the bacterial colonies changed from 1329 to 56. The titania photokilling activity is dominant. A detailed explanation of photokilling activity for *E. coli* cells was presented by Sunada et al. [27]. They explained that the *E. coli* cell wall acts as an outer barrier that hinders initial photokilling. The process is described by a two-step decay chain for the survival rate of *E. coli* on a titania film [28].

*3.2. Silver nanoparticle-decorated soy protein-based nanofibers*

Soy protein/nylon 6 nanofibers were decorated with silver nanoparticles as follows. Two different $AgNO_3$ solutions in water were prepared: 4 wt.% (to be termed as solution A) and 1 wt.% (to be termed as solution B). Collected soy protein-containing nanofibers were immersed in solutions A or B and then left at room temperature for 24 h to dry. Sample weights were measured before and after immersion and drying. Both sets of samples revealed an increase in their weights since silver ions were deposited onto nanofiber surfaces. The average weight increase after the sample immersion in 1 and 4 wt.% $AgNO_3$ solutions was 6.38 ± 2.93% and 45.15 ± 20.60%, respectively.

Then, two different post-treatments of the samples were used. In the first-type of treatment nanofibers soaked in solutions A or B were subjected to a reducing agent solution (1 wt% $NaBH_4$ solution in water). This was done to reduce $AgNO_3$ to silver nanoparticles embedded in nanofibers. After the addition of $NaBH_4$ solution to the nanofibers, the samples were left at room temperature to dry out completely. The post-treated nanofibers thus obtained will be denoted

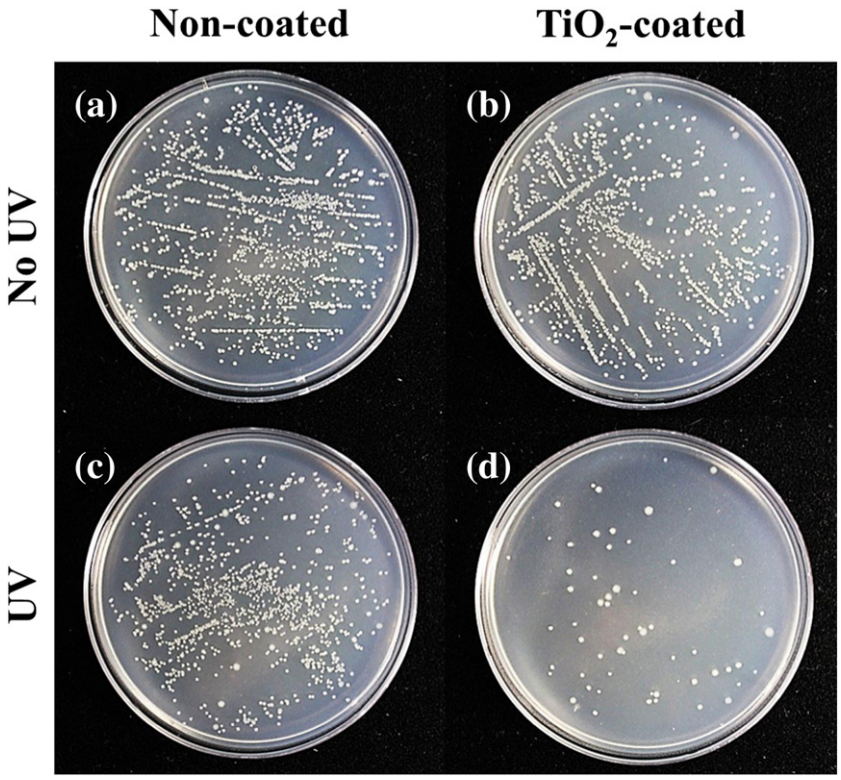


**Fig. 3.** Inhibition of *E. coli* by titania-decorated nanofiber mats. The UV light exposure time was 1 hour.

as Ar and Br. The adding of the reducing agent resulted in an additional increase in the sample weight accompanying formation of silver nanoparticles on the nanofiber surfaces after the immersion in 1 wt.% $NaBH_4$ solution and drying: 30.43 ± 4.31% for soy protein nanofibers not decorated with silver, 121.21 ± 29.15 % for 1 wt.% $AgNO_3$-treated soy protein nanofibers, and 115.61 ± 41.51 % for 4 wt.% $AgNO_3$-treated soy protein nanofibers. For control, samples of soy protein nanofiber mats from the same batch which did not undergo treatment with $AgNO_3$ were also immersed in 1 wt.% aqueous solution of sodium borohydride ($NaBH_4$) and it was found that their weight also increased as mentioned above. These results demonstrate that formation of silver nanoparticles is accompanied by deposition of some other materials at the nanofiber surfaces.

As the second post-treatment the nanofibers soaked in solution A were heat-treated at a temperature of 120 °C to thermally decompose $AgNO_3$ to the embedded silver nanoparticles. These post-treated samples are denoted as Ah. The SEM images of these three different types of samples obtained using variable pressure Hitachi S-3000N are shown in Fig. 4. In particular, Fig. 4**a** shows the SEM image of sample Ar, Fig. 4**b** — sample Br, and Fig. 4**c** — sample Ah. It is seen that sample Ar is completely covered with silver nanoparticles, whereas for sample Br the coverage with silver nanoparticles is less than that of sample Ar. This can be attributed to the fact that sample Ar was prepared using solution A with higher concentration of $AgNO_3$. Fig. 4**c** shows that sample Ah is covered with silver films rather than silver nanoparticles which cover samples Ar and Br. Note that these differences were also evident from visual observations as a different sample color. Namely, sample Ar was dark brown, sample Br was light brown, and sample Ah was dark yellow (cf. Fig. 5). In the following it will be shown that the effect of such variations in sample structure has a pronounced effect on their antimicrobial activity.

In order to evaluate longevity of silver nanoparticles embedded in nanofiber mats as anti-microbial agents, their leaching when exposed to water over long periods of time should be investigated. In ref. [29] it was shown that about 99% of silver nanoparticles decorated on the surface of silica nanofibers and treated by UV were left intact after 24 h of exposure to water. Silver ions release profile from poly (L-Lactide), PLA, fibers has been reported in ref. [30] where atomic absorption spectroscopy was used. Ag/PLA samples were immersed in phosphate buffered saline and after equal time intervals the solution was tested for the traces of silver ion in it. The cumulative released amount was less than 500 ppm over 20 days of release for 32 wt.% $AgNO_3$/PLA. In ref. [31] silver nanoparticles were deposited on polyester and polyamide fabrics and laundering durability of silver-coated samples after five consecutive washing cycles was investigated. Before undergoing washing steps, samples revealed 99.9% of bacterial removal, whereas this value was reduced to 85.3% after five cycles of washing, which indicates the degree of leachability of silver nanoparticles which act as an antibacterial agent. Release profile of silver ions from extruded polyamide was measured in ref. [32]. Silver-coated samples were immersed in water and water samples were collected to analyze for the presence of silver ions at specified time intervals using atomic absorption spectroscopy. It was concluded that the release rate increases over time.

In order to evaluate silver leaching from soy protein nanofiber mats, samples which were treated with sodium borohydride solution and decorated with silver nanoparticles were immersed in 10 ml of de-ionized water for 24 h. Then they were extracted and left for drying. The control samples without silver nanoparticles but dipped into sodium borohydride solution underwent a similar immersion in water for 24 h and drying. The weight loss in water for 24 h of all these samples was found as: 34.99 ± 6.52 % for soy protein nanofibers not decorated with silver, 41.72 ± 5.77 % for 1 wt.% $AgNO_3$-treated soy protein nanofibers, and 40.33 ± 9.74% for 4 wt.% $AgNO_3$-treated soy protein nanofibers. Most of these weight losses can be attributed to the materials deposited on the nanofibers during treatment with sodium borohydride (listed before). Only the difference in the weight loss between silver-decorated and non-decorated nanofibers could be attributed to silver leaching. However, the difference does not exceed the statistical variance, which leads to the conclusion that no measurable silver leaching was detected.

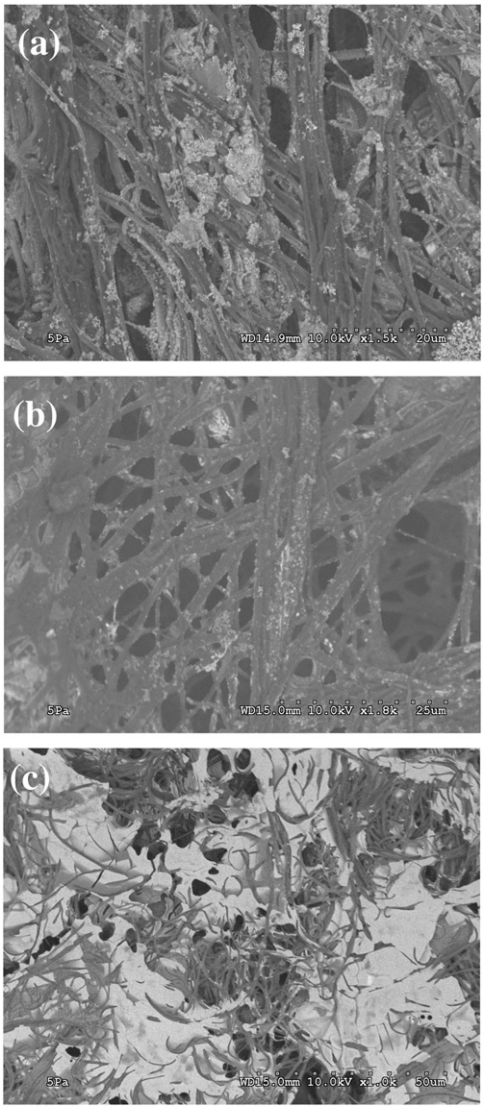


**Fig. 4.** SEM images of samples (a) Ar, (b) Br and (c) Ah. It is seen that sample Ar and Br are coated with the embedded silver nanoparticles and their clusters, whereas sample Ah is covered with silver films (silver is visible as light spots in the images). The comparison of panels (a) and (b) shows that the coverage of sample Ar with silver nanoparticles is larger than the coverage of sample Br.

An agar-filled Pyrex Petri dish was divided into four equal areas. Three thin round samples of silver-decorated nanofiber mat and a control nanofiber sample with no silver were gently pressed onto the agar surface and the inoculum. All four samples had an approximately equal area. The Petri dish was incubated at 37 °C overnight. The antibacterial activity was determined by the clear zones around the silver-decorated nanofiber samples. The absence of cell culture in a certain area near a sample was considered as an evidence of the inhibition of bacterial growth (Fig. 5). No clear area around the control sample 4 is visible which shows that the inhibition of *E. coli* is associated solely with silver nanoparticles. Fig. 5 shows that the magnitude of the clear area around the samples corresponds in the descending order to samples Ar, Br, and Ah. This means that the antibacterial activity of sample Ar was stronger than those of samples Br and Ah and, correspondingly, it was inhibiting the growth of *E. coli* stronger. This phenomenon is attributed to the differences in silver coverage of these samples. It is known that nanoparticles possess a higher antimicrobial activity than macroscopic objects owing to their high surface area to volume ratio. That is why samples Ar and Br are more active than sample Ah. Also, sample Ar is more active than Br because of the higher coverage of silver nanoparticles on the former. It is emphasized that the antibacterial activity of silver-decorated nanofiber mats does not require any UV irradiation.

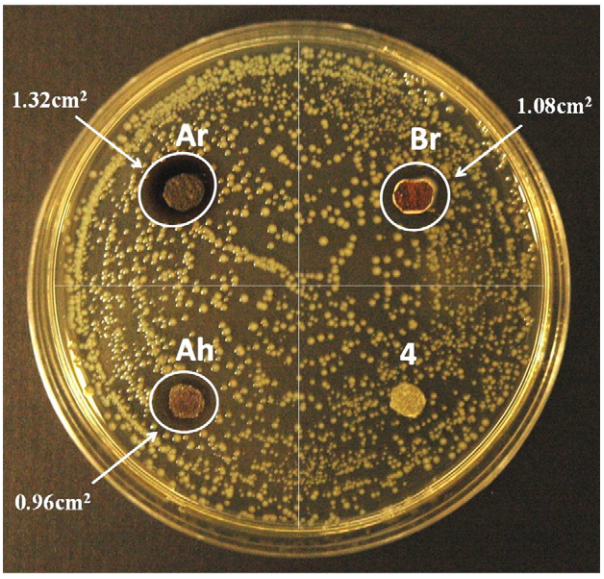


**Fig. 5.** Inhibition of *E. coli* by silver-decorated soy protein nanofiber mats. The area of the clear areas around the nanofiber mat samples 1, 2 and 3 were 1.32 $cm^2$, 1.08 $cm^2$ and 0.96 $cm^2$, respectively. No clear area and thus inhibition is seen around the control nanofiber mat 4 (with no silver).

## 4. Conclusions

In this work two different system of antimicrobial substrates based on polymer nanofibers were studied: (a) electrospun nylon 6 nanofibers decorated with $TiO_2$ nanoparticles, and (b) solution-blown soy protein-based nanofibers coated with silver nanoparticles. The rate of electrospinning is much lower than that of the solution blowing and the inter-fiber pore size in electrospun mats is smaller than that in the solution-blown mats, which are fluffier. It was found that $TiO_2$ decorated antimicrobial nanofibers inhibit growth of *E. coli* and kill them under UV light. On the other hand, soy protein nanofibers decorated with silver nanoparticles do not require any UV light activation because of the inherent antimicrobial activity of silver nanoparticles, which is demonstrated in the experiments in this work. Possible silver leaching was tested, and no reliable evidence of it was found in 24 h. These two different antibacterial nanofibers can be combined in water purification industry as the materials used for making nanofibers are not soluble in water. In addition, nanofibers prepared in this work are biocompatible, which allows using them in bandages for wound healing.

## Acknowledgements

This work was supported by a research contract with the United Soybean Board, Chesterfield, Missouri (research contract no. 0491). Help of Dr. Wonhwa Cho and Marian Fernando (UIC) is greatly appreciated. This work was also supported by National Research Foundation of Korea (2012-0001169, 2011-0030433, and 2010-0010217), and the Converging Research Center Program (2010K000969). This study was also supported by a grant from the cooperative R&D Program (B551179-08-03-00) funded by the Korea Research Council Industrial Science and Technology and by World Class University (WCU) program (Case III, NRF, R33-10046).

## References


[1] C. Mccullagh, J.M.C. Robertson, D.W. Bahnemann, P.K.J. Robertson, Research on Chemical Intermediates 33 (2007) 359–375.
[2] D. Qi, X. Kang, L. Chen, Y. Zhang, H. Wei, Z. Gu, Analytical and Bioanalytical Chemistry 390 (2008) 929–938.
[3] S.-y. Lu, D. Wu, Q.-l. Wang, J. Yan, A.G. Buekens, K.-f. Cen, Chemosphere 82 (2011) 1215–1224.
[4] M.N. Charis, H.S. Cheng, A.D. Aleksandra, A.M.C. Ng, C.C.L. Fredrick, W.K.J. Chan, Applied Polymer Science 122 (2011) 1572–1578.
[5] K. Kawata, M. Osawa, S. Okabe, Environmental Science and Technology 43 (2009) 6046–6051.
[6] B. Zielinska, J. Grzechulska, A.W. Morawski, Journal of Photochemistry and Photobiology A: Chemistry 157 (2003) 65–70.
[7] K. Kabra, R. Chaudhary, R.L. Sawhney, Industrial and Engineering Chemistry Research 43 (2004) 7683–7696.
[8] Z.S. Pillai, P.V. Kamat, Journal of Physical Chemistry 108 (2004) 945–951.
[9] A. Markowska-Szczupaka, K. Ulfig, A.W. Morawski, Catalysis Today 169 (2011) 249–257.
[10] K. Tanaka, K. Padermpole, T. Hisanaga, Water Research 34 (2000) 327–333.
[11] Y. Wang, Water Research 34 (2000) 990–994.
[12] R.P.S. Suri, J. Liu, D.W. Hand, J.C. Crittenden, D.L. Perram, M.E. Mullins, Water Environment Research 65 (1993) 665–673.
[13] K.B. Sherrard, P.J. Marriott, R.G. Amiet, R. Colton, M.J. McCormick, G.C. Smith, Environmental Science & Technology 29 (1995) 2235–2242.
[14] M. Hamerski, J. Grzechulska, A.W. Morawski, Solar Energy 66 (1999) 395–399.
[15] D.M. Blake, P.C. Maness, Z. Huang, E.J. Wolfrum, J. Huang, W.A. Jacoby, Separation and Purification Methods 28 (1999) 1–50.
[16] I.J. Ochuma, O.O. Osibo, R.P. Fishwick, S. Pollington, A. Wagland, J. Wood, J.M. Winterbottom, Catalysis Today 128 (2007) 100–107.
[17] D.H. Reneker, A.L. Yarin, Polymer 49 (2008) 2387–2425.
[18] X.-H. Qin, S.-Y. Wang, Journal of Applied Polymer Science 102 (2006) 1285–1290.
[19] J. Doshi, D.H. Reneker, Journal of Electrostatics 35 (1995) 151–160.
[20] P. Zahedia, I. Rezaeiana, S.-O. Ranaei-Siadatb, S.-H. Jafaria, P. Supaphol, Polymers for Advanced Technologies 21 (2010) 77–95.
[21] J.-J. Park, J.-G. Lee, D.-Y. Kim, J.-H. Hong, J.-J. Kim, S. Hong, S.S. Yoon, Environmental Science & Technology 46 (2012) 12510–12518.
[22] S. Sinha-Ray, Y. Zhang, A.L. Yarin, S. Davis, B. Pourdeyhimi, Biomacromolecules 12 (2011) 2357–2363.
[23] S. Khansari, S. Sinha-Ray, A.L. Yarin, B. Pourdeyhimi, Journal of Applied Physics (2012) 111.
[24] C. Yogi, K. Kojima, N. Wada, H. Tokumoto, T. Takai, T. Mizoguchi, H. Tamiaki, Thin Solid Films 516 (2008) 5881–5884.
[25] T. Zhang, T. Oyama, A. Aoshima, H. Hidaka, J. Zhao, N. Serpone, Journal of Photochemistry and Photobiology A: Chemistry 140 (2001) 163–172.
[26] Y. Sakatani, D. Grosso, L. Nicole, C. Boissière, G.J. de AA Soler-Illia, C. Sanchez, Journal of Materials Chemistry 16 (2006) 77–82.
[27] K. Sunada, T. Watanabe, K. Hashimoto, Journal of Photochemistry and Photobiology A: Chemistry 156 (2003) 227–233.
[28] K. Sunada, T. Watanabe, K. Hashimoto, Environmental Science & Technology 37 (2003) 4785–4789.
[29] K.D. Min, W.H. Park, J.H. Youk, Y.-J. Kwark, Macromolecular Research 16 (2008) 626–630.
[30] X. Xu, Q. Yang, Y. Wang, H. Yu, X. Chen, X. Jing, European Polymer Journal 42 (2006) 2081–2087.
[31] M. Radetic, V. Illic, V. Vodnik, S. Dimitrijevic, P. Jovancic, Z. Saponjic, J.M. Nedeljkovic, Polymers for Advanced Technologies 19 (2008) 1816–1821.
[32] R. Kumar, H. Munstedt, Biomaterials 26 (2005) 2081–2088.